Composite modular floor prototype for emergency housing applications: finite element approach

Hassan Abdolpour[a, 1], Julio Garzón-Roca[b], Gonçalo Escusa[a],

José M. Sena-Cruz[a,], Joaquim A.O. Barros[a], Isabel B. Valente[a]

[a] ISISE, University of Minho, Guimarães, Portugal

[b] Department of Geotechnical and Geological Engineering, Universitat Politècnica de València, Valencia, Spain

Abstract

The paper presents the numerical modelling of a temporary residential floor prototype composed of three jointed composite floor sandwich panels made of glass fiber reinforced polymer (GFRP) skins, a polyurethane foam core (PU) and pultruded U-shaped GFRP profiles working as ribs. Panels are supported on a GFRP pultruded frame structure. A 3D nonlinear finite element model is developed considering geometrical and material nonlinearities and adherent surfaces interaction. The model is coherently validated with experimental results, showing its capability to capture the mechanical performance of a single panel (which includes the possibility of local instability on the GFRP skin), two and three panels working together, and the whole prototype. A series of parametric studies are then conducted using the numerical model developed. Those studies aim to (i) assess the influence that ribs on the panel stiffness and on the shear stresses distribution through the sandwich panel's components, (ii) the flexibility of the designed connections between jointed panels and frame structure, and (iii) the influence of geometry in the modular housing.

Keywords: emergency house; composite materials; GFRP pultrude profiles; sandwich panel; GFRP skins; PU foam core; FE model.

---

[1] Corresponding author. Tel.: +351-253-510-200; fax: +351-253-510-217

  E-mail address: Hassan.abdolpour@gmail.com (H. Abdolpour)

1. Introduction

Temporary residential buildings are needed for different purposes, such as: settling down local communities that were displaced after natural disasters, offices or storages of construction equipment in construction sites, additional public portable school classroom space and accommodation for tourists and professionals in the case of special events. Reducing construction time and producing lightweight structures to be easily transported to the affected areas, with an effortlessly assemblage/disassemblage are one the main issues confronted in the engineering field [1]. One way forward to these goals is to adopt an industrial building process with increased prefabrication and modularity [2]. Moreover, the use of materials with good resistance in both mechanical and environmental terms is also highly desired. Due to the characteristics and efficiency of fibre reinforced polymers (FRP), these composite materials have been attracted by a variety of industrial sectors [3]. Hence, the use of sandwich panels made of FRP materials emerges as a potential solution for these light structural applications.

A sandwich structure is a special form of laminated composite materials that combines two thin and stiff skins separated by a thick and lightweight core material [4]. These components are attached together using adhesives [5]. In a sandwich structure, bending loads are carried by the skins while shear loads are resisted by the core [6]. Furthermore, the core material should stabilize the skins against buckling and wrinkling. The bond between skins and core must have sufficient strength to withstand the shear and the tensile stresses introduced between them. The main advantage of composite sandwich panels is a high bending stiffness and a high strength to weight ratio [7]. Furthermore, sandwich elements present higher corrosion resistance than other conventional materials [8].The efficiency of composite sandwich panels was investigated by different researchers in various applications: cladding [9], facades [10, 11], roofing [12] , walls [13] and emergency housing [14]. Different techniques for connecting FRP panels in modular housing systems [15, 16] and bridge decks [17-21] are documented in the literature.

A number of modeling techniques have also been developed, including analytical models and numerical approaches. Ha [22] reviewed the existing finite element (FE) techniques for analyzing sandwich plates. The summarized models in this study, varied from simple 3DOF (degree of freedom) per node in symmetric three-layer sandwich plates comprising flexible core and thin face skins to complex layered elements for sandwich construction with multi thin face skins and core. Thomsen [23] achieved a good match between an approximate method and the finite element method in the analysis of local bending stresses and displacement in sandwich

plates composed of orthotropic face skins and core. In this study, elastic foundation was used by considering face skins with orthotropic linear elastic behavior and the core material with isotropic linear elastic behavior. Hyer et al. [24] compared the results of simple sandwich plate theory with the experimental tested sandwich plates simply supported along two edges and loaded by a line load. A satisfactory correlation was obtained in this comparison. Demiray et al. [25] developed a triangular finite element with three nodes on each skin using the Newton-Raphson method for solving the nonlinear discretized problem. It was deduced that the local wrinkling of the skin corresponded to the core compressibility. Tuwair et al. [26] evaluated the behavior of sandwich panels with various foam core and ribs configuration, through experimental testing. The tested specimens were manufactured using pultrusion method. The experimental program was validated with FEM simulations, by using 3D hexahedral deformable solid elements for the sandwich panel's components. Interaction between skins and core was defined as a full composite. The same methodology was used in other studies, but considering a cohesive zone model to define the interaction between skins and core [27-29].

Continuing the work developed by the authors [16, 30], the present paper presents a comprehensive numerical analysis of a composite prototype to be used as the floor module of an emergency house. The architectural aspect of the proposed emergency house is represented in **Fig. 1.** This emergency house was developed in the scope of ClickHouse project.

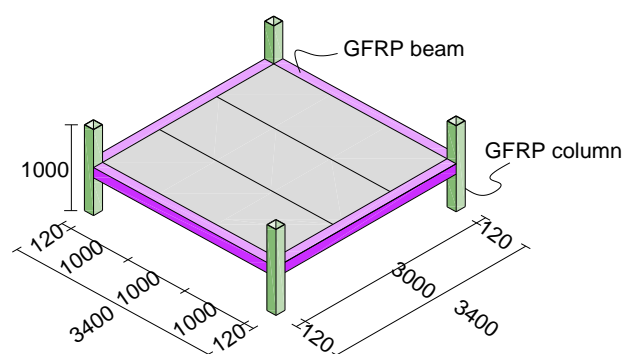**Fig. 1**. Architectural aspect of the temporary housing system.

The house is mainly composed of three blocks whose enclosure surfaces are sandwich panels of GFRP skins and PU foam core. Panels are supported on GFRP beams and columns, which act as a frame structure. An

experimental program was conducted [31] in a previous phase of the work in order to assess the mechanical behavior of the sandwich panels and the floor prototype, and to perform a complete material characterization. In this paper, those experimental results are used to calibrate and validate a nonlinear three-dimensional finite element model, which takes into account different constituent models for the sandwich panels components, as well as a cohesive interaction model between the adherent surfaces of the panel. The FE model is later used to carry out a series of parametric studies. These parametric studies aim to analyse the influence of: (i) placing internal ribs on the sandwich panels, (ii) the flexibility of the connection between panels and the frame structure, and (iii) the influence that aspect ratio and slender ratio can have in the design of these structures. Sandwich panel aspect ratio, r, is defined as L/w, where L and w are the panel's length and width, respectively. Slender ratio, r_s, is defined as h/w, where h is the height of the sandwich panel.

2. Summary of the previous experimental program

The floor prototype tested in the experimental program [31]consisted of a frame structure and three floor panels configuring the slab. Geometry of the different components of the prototype, as well as details on the connections, are shown in **Fig. 2.** The frame structure comprised beams and columns formed by tubular pultruded GFRP profiles (**Fig. 2**a). Floor panels were designed as composite sandwich panels, with a low density polyurethane (PU) foam core enclosed by two thin GFRP skins (**Fig. 2**b). Each panel contained U-shaped GFRP pultruded profiles on each edge to enable connection of panels with beams and other panels. Two additional U-shaped profiles were placed inside the core, working as ribs, to increase flexural and shear stiffness (**Fig. 2**c).

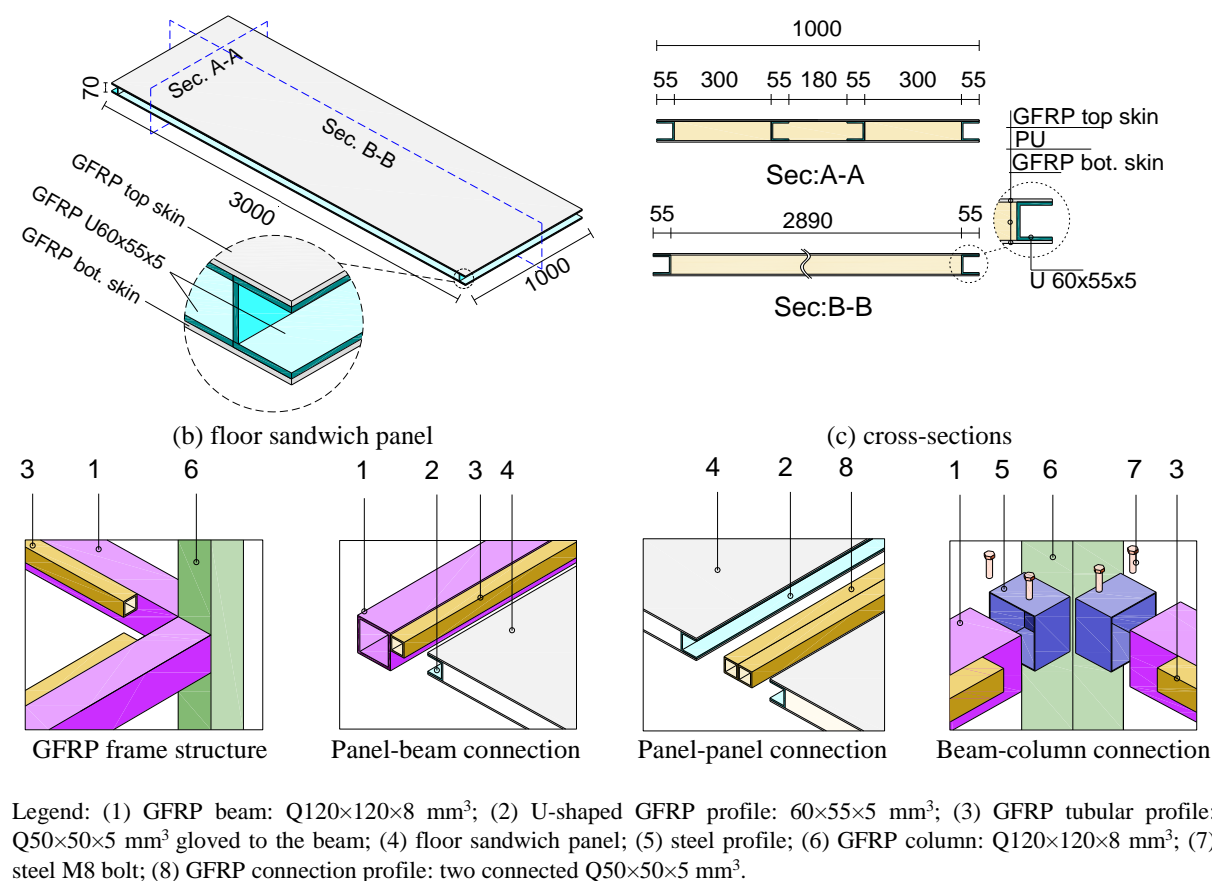

(a) unit of floor modular prototype

(b) floor sandwich panel   (c) cross-sections

GFRP frame structure   Panel-beam connection   Panel-panel connection   Beam-column connection

Legend: (1) GFRP beam: $Q120 \times 120 \times 8$ mm^3; (2) U-shaped GFRP profile: $60 \times 55 \times 5$ mm^3; (3) GFRP tubular profile: $Q50 \times 50 \times 5$ mm^3 gloved to the beam; (4) floor sandwich panel; (5) steel profile; (6) GFRP column: $Q120 \times 120 \times 8$ mm^3; (7) steel M8 bolt; (8) GFRP connection profile: two connected $Q50 \times 50 \times 5$ mm^3.

Fig. 2 Schematic representation of the emergency house components and floor prototype tested (all units in mm).

Characterization tests on the different involving materials were perfomed, (i) including tensile tests on GFRP skins and beams; (ii) compression, tension and shear tests on the PU foam; and, (iii) pull-off tests to evaluate bond between GFRP skin and PU foam. The mechanical response of the prototype was assessed through a series of flexural tests on: a single panel, two and three panels working together (hereafter called "jointed panels"), and the whole floor prototype. Service load was set to be equal to 1.6 kN/m^2 in the developed tests, in accordance with United Nations (UN) recommendations for temporary houses [32]. That load was increased 1.5 times to evaluate ultimate limit state (ULS) of panels, as defined in Eurocode 0 [33].

A four-point bending test (4PBT) on a single sandwich panel (**Fig. 3a**) was carried out to study its behaviour up to failure, according to ASTM C393 standard [34]. For this test, the shear span was set to 850 mm and the total clear span is equal to 2700 mm. Supports consisted in steel rollers placed at both ends and under the panel. Those supports allowed free rotation and one of them also allowed longitudinal sliding. The 4PBT configuration was also used to test two series of two jointed panels and one series of three jointed panels in a similar test setup that is indicated in **Fig. 3b**. Shear and clear span, as well as support conditions, were identical to the single panel

test described before. Tests on jointed panels were performed until reaching the ULS load. The whole floor prototype behaviour was evaluated by imposing a uniform load on ULS condition (i.e. 2.4 kN/m^2). The prototype was loaded by using a swimming pool with circular area of 6.25 m^2, filled with 2160 litters of water (**Fig. 3c**).

In all the tests referred, vertical deflections and strains on GFRP skins and beams were measured, along with the load application, by using LVDTs and strain gauges respectively. Monitoring involved a total of 15 LVDTs and 16 strain gauges. Instrumentation was placed at midspan of the panels, at connections between panels, under loaded sections and at the frame beams. More information about the tests described above can be found in [31].
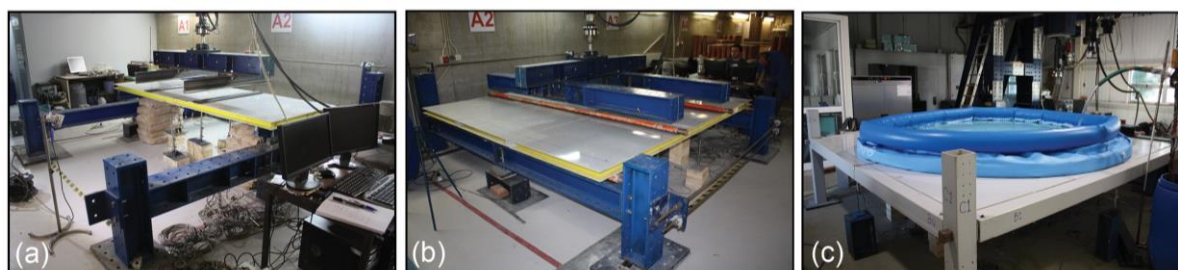

Fig. 3 Flexural tests setup: (a) four-point bending test (4PBT) on single panel up to failure; (b) 4PBT on three jointed panels; and (c) floor prototype under uniform loading.

3. Finite element model

Nonlinear three-dimensional finite element models were developed to simulate the behaviour of a single panel, two jointed panels, three jointed panels and the full prototype. These models were developed considering all the geometrical and material information gathered in the physical models and the experimental tests described in the previous section. The FE simulations were developed using the commercial software ABAQUS v6.12 [35]. A nonlinear static analysis enabling geometric nonlinearities based on the direct Full Newton-Raphson Technique was used to run the simulations.

3.1. Finite elements, mesh description, boundary conditions and loading

All sandwich panel constituents, i.e. GFRP skins, PU foam core, GFRP U-shaped profiles and GFRP connection profiles, as well as the frame components (GFRP beams and columns), were modelled using 3D hexahedral deformable solid elements, with 8 nodes and 3 degree of freedom per node (C3D8). After some preliminary analyses, it was found that elements with an approximate size of 50 mm of side were optimal in terms of accuracy, convergence and computational time of the simulation. A schematic representation of the finite elements models developed is represented in **Fig. 4**.

Due to the symmetry of panels and loading conditions, and with the aim of reducing time of analysis, only one quarter of the structure was simulated in the case of the single panel and the jointed panels (see **Fig. 4**). Corresponding boundary conditions in the symmetry planes were applied, as well as a roller support condition at the end of the panels, under the bottom skin. In order to simulate the 4PBT configuration, a vertical displacement was imposed to the nodes positioned along a loading line located similarly to the experimental tests.

Similarly, one-quarter of the structures was simulated in the case of the floor prototype (see **Fig. 4**). The vertical displacement and one horizontal displacement were fixed on the column, in the virtual contact with the pavement. A uniform load of 2.4 kN/m^2 was applied on the top surface of the sandwich floor panels. This load was previously justified in Section 2.
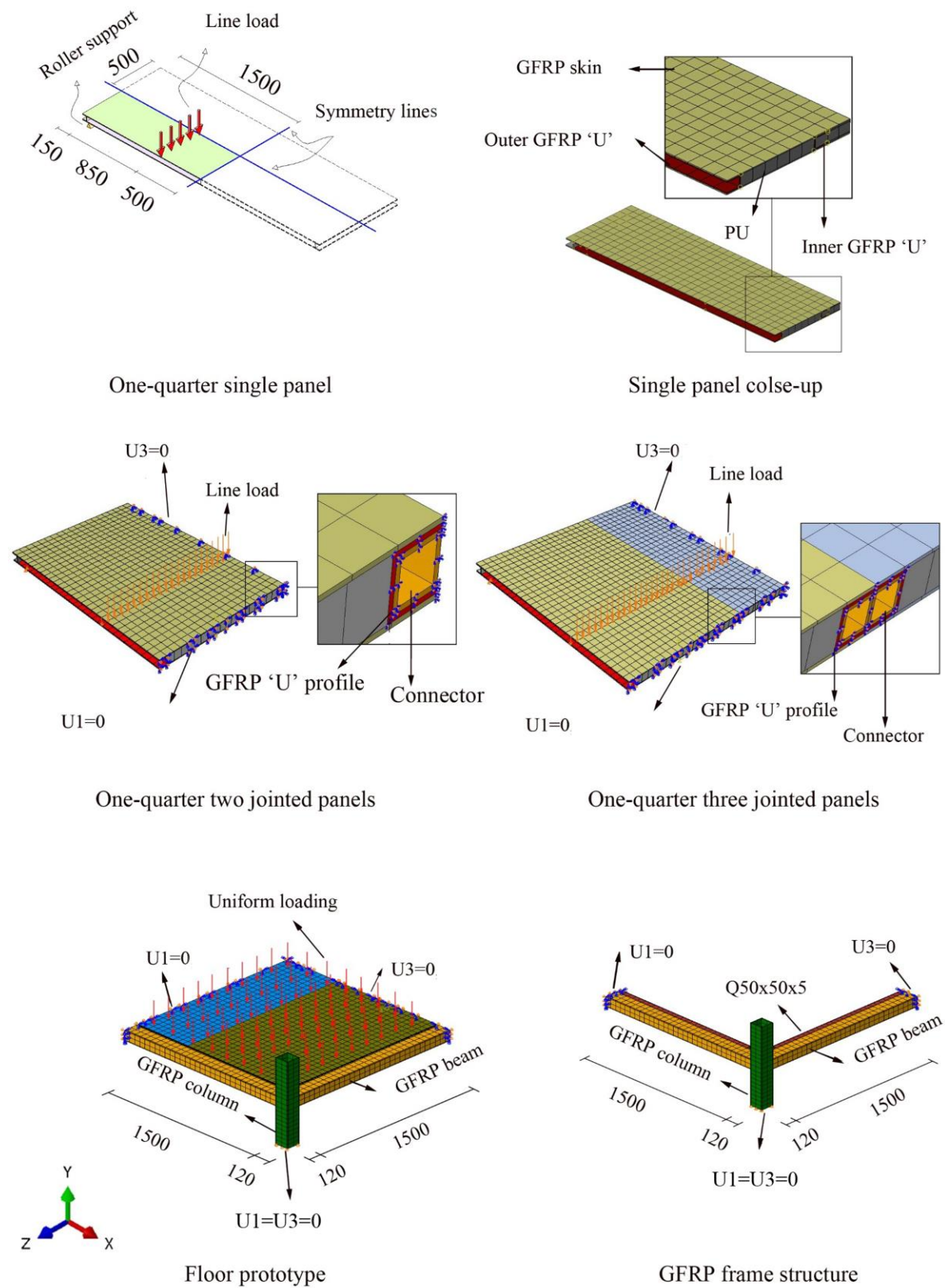
Fig. 4. FE model details.

3.2. Constitutive models and interaction between the different panel components

Table 1 includes information about the constitutive models applied to each material involved in the simulations and summarizes the parameters that define each model. Material properties were adopted according to the characterization tests performed on the components that comprise the prototype [31]. As the GFRP skins had a quasi-isotropic lay-up, an isotropic linear elastic material with maximum normal tensile stress was chosen to represent the GFRP skin mechanical behaviour. The PU foam core was simulated as crushable foam, based on the results previously obtained by other authors [36]. All GFRP pultruded profiles, which include ribs, connection profiles and frame beams and columns, were modelled assuming a linear-elastic orthotropic material model, with different elastic properties and ultimate tensile stresses in parallel to the fiber direction (longitudinal direction), and perpendicular to the fiber direction (transverse).

Table 1. Constituent models for sandwich panels components

Component		GFRP Skins	PU foam core	GFRP profiles (ribs, connection profiles, beams and columns)
Constitutive model		Isotropic linear-elastic	Crushable foam	Orthotropic linear-elastic
Poisson coefficient	(-)	0.30	0.15	0.30
Elastic modulus	(MPa)	9600	6	-
Elastic modulus (longitudinal)	(MPa)	-	-	32000
Elastic modulus (transverse)	(MPa)	-	-	13000
Ultimate tensile stress	(MPa)	117	0.49	-
Ultimate shear strength	(MPa)	-	0.15	-
Compressive yield stress	(MPa)	-	0.30	-
Ultimate tensile stress (longitudinal)	(MPa)	-	-	415
Ultimate tensile stress (transverse)	(MPa)	-	-	180

Interaction between all adherent surfaces belonging to a panel, i.e. interfaces between PU and GFRP skins, PU and U-shaped GFRP profiles, and GFRP skins and U-shaped GFRP profiles, were modelled as cohesive [37]. The generalized cohesive-behaviour included in the ABAQUS package was used. This is a surface-based cohesive behaviour defined by a traction-separation law (**Fig. 5a**). The model considers linear-elastic behaviour until reaching a certain value of interface stresses (t) and surface separation (δ). Afterwards, initiation and

evolution of damage occurs. The elastic behaviour of the model is written in terms of an elastic constitutive matrix that relates the normal and shear stresses (referred to as traction t) to the normal and shear separation across the interface(δ). Thus, surface separation (δ) is computed by Eq. (1)

$$[t] = [k][\delta] \tag{1}$$

Associated cohesive elements contain three components (**Fig. 5b**): two shear forces parallel to the plan of interaction (s_1 and s_2) and a normal force (n) to the interaction plane. Accordingly, Eq. (1) could be written in the form of Eq. (2):

$$\begin{bmatrix} t_n \\ t_{s_1} \\ t_{s_2} \end{bmatrix} = \begin{bmatrix} k_{nn} & k_{ns} & k_{ns_2} \\ k_{ns_1} & k_{s_1s_1} & k_{s_1s_2} \\ k_{ns_2} & k_{s_1s_2} & k_{s_2s_2} \end{bmatrix} \begin{bmatrix} \delta_n \\ \delta_{s_1} \\ \delta_{s_2} \end{bmatrix} \tag{2}$$

In the simulation, an uncoupled behaviour was assumed between the tractions and separations. This means that the stress in the normal direction did not result in a separation in the shearing directions and shear stress did not lead to any separation in the normal direction. Therefore, in the stiffness matrix $[k]$, the off-diagonal components were considered to be zero.
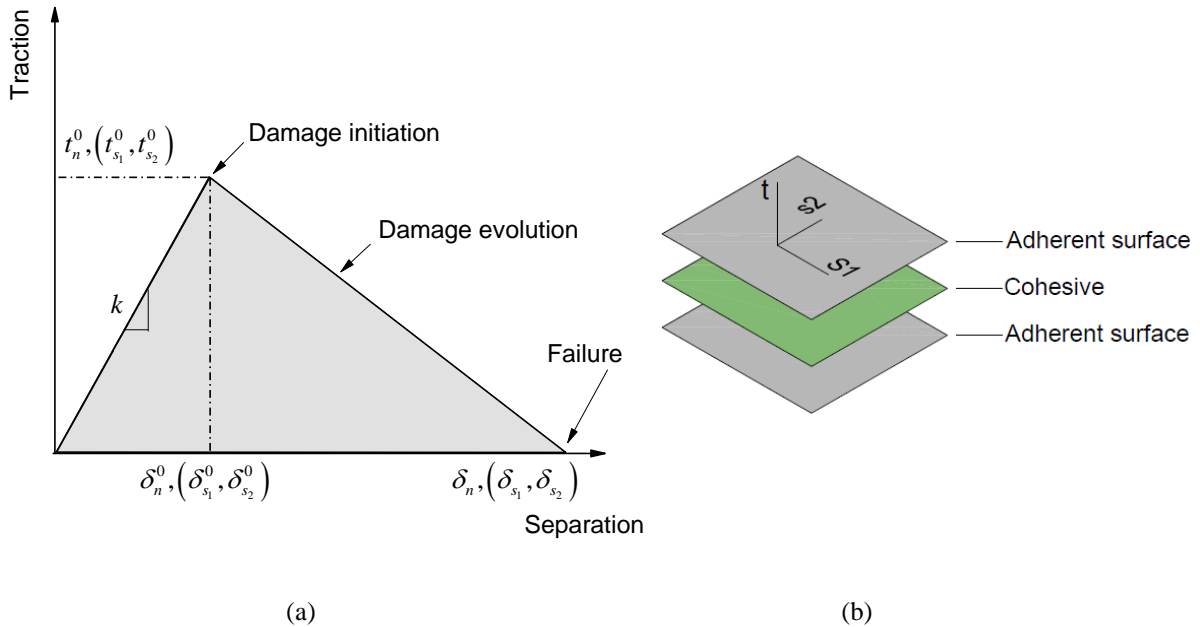

(a)   (b)

Fig. 5. Cohesive behaviour simulated: (a) traction-separation response; (b) cohesive element.

Degradation of bond between two adherent surfaces is simulated with a damage model. Initiation of damage was defined by a stress based traction separation law, and it was assumed that failure mode corresponds to an "opening" (see **Fig. 6**), according Westergaard [38]. No mode-mixity was taken into account for simplicity. Consequently, damage initiated in the model, when the maximum contact stress ratio reached one of the maximum values presented [28] by Eq. (3):

$$\max\left[\frac{\langle t_n \rangle}{t_n^0}, \frac{t_{s_1}}{t_{s_1}^0}, \frac{t_{s_2}}{t_{s_2}^0}\right] = 1 \tag{3}$$

where t_n is the normal stress; t_{s_1} and t_{s_2} are the shear stresses (in planes s_1 and s_2); and t_n^0, $t_{s_1}^0$ and $t_{s_2}^0$ represent the peaks for normal stress and shear stresses (in planes s_1 and s_2), respectively.
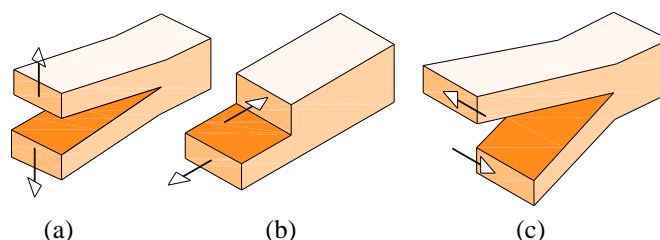

Fig. 6. Failure modes: (a) opening; (b) sliding; (c) shearing

Since in the direct pull-out tests it was demonstrated [31] that the stiffness degradation between GFRP material and PU foam was due to failure of the foam itself, the peak value were substituted by the maximum tensile strength and maximum shear strength of the foam core, as indicated in **Table 1**. It is worthwhile mentioning that mode-mixity was not presumed in this simulation, and therefore, defining the shear stress value did not have any influence on the type of simulation, even though ABAQUS requires those values [29].

Finally, a damage evolution law was defined. For the evolution of the initiated damage, an energy based approach with a linear softening law was utilized. Fracture energy of 0.01 J/m^2 was adopted for the simulations according to the other performed research findings [29].

3.3. Panel-panel and panel-beam connections

Connections between panels and between panels and beams were modelled with interfaces. Behaviour in normal direction was modelled as "hard" contact (ABAQUS [35]), meaning that no penetration was allowed between the two surfaces and there was no limit to the magnitude of contact pressure transmitted when the surfaces were in contact. Behaviour in tangential direction was modelled by the classical Coulomb friction law, but without

any contact cohesion. A trial and error calibration of the model against the experimental results led to set the

friction coefficient equal to 0.10.

4. Model validation

4.1. Single panel up test to failure

Error! Reference source not found.**a** shows the load-midspan deflection curve obtained from the FE simulation

plotted against the experimental result, while the load-strain response in the GFRP skins, at the middle of the

panel registered experimentally and numerically is showed in Error! Reference source not found.**b**. A very good

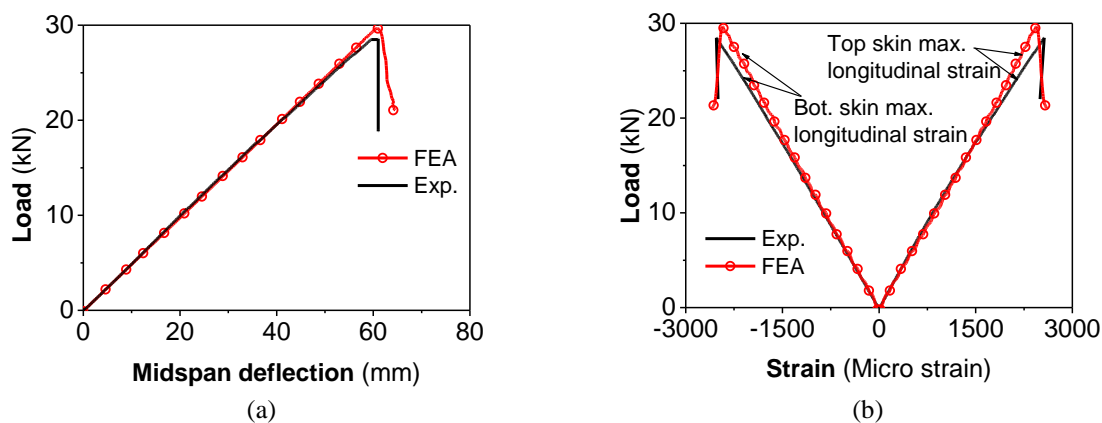match is observed between the numerical results obtained by the FE model developed and the experimental

ones.

Fig. 7 Experimental *versus* FE simulation in single sandwich panel: (a) load *versus* midspan deflection; (b) load *versus* strain.

The FE model accurately captured the single sandwich panel's flexural behaviour. The panel failed at a

maximum load of 28.47 kN (29.66 kN in the FE model) registering a midspan deflection of 61.02 mm

(60.83 mm in the FE model) with a robustly linear behaviour prior to the abrupt failure. Experimentally, failure

was caused by a localized debonding between the GFRP compression skin (top skin) and the PU foam core (**Fig.**

8a). Failure occurred at the region of maximum flexural moment, between the two lines of loading [39]. This

phenomenon, known as local instability or wrinkling failure mode of sandwich panels, led to a sudden outward

buckling of the GFRP skin in the compression side [4, 40, 41]. Similar failure mode was predicted by the FE

model (**Fig. 8**b).
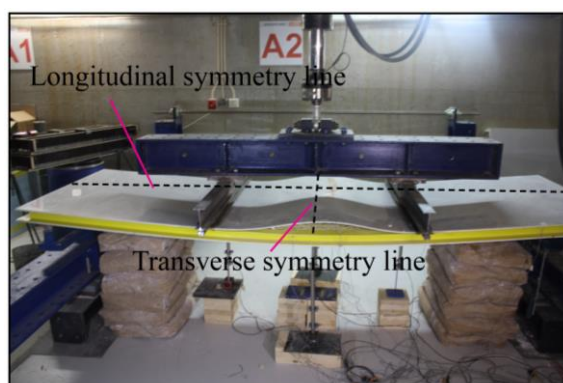
(a)
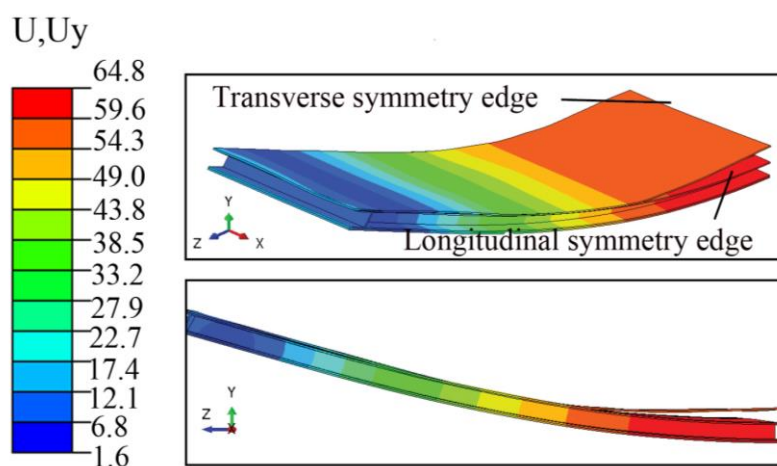
(b)

Fig. 8. Failure mode in single panel: (a) experimental; (b) FE simulation (units are in mm).

4.2. Jointed panels

This section presents the results obtained in the models with two jointed panels and three jointed panels. Accordingly, **Fig. 9** compares the results obtained by the FE model with the experimental ones. Note that values plotted for deflection and strain correspond to an average of those values registered experimentally and numerically at the center of the panels. As can be seen, the FE models successfully reproduce the flexural performance of jointed panels. As aforementioned, the jointed panels were tested in SLS loading conditions, hence failure did not occur.
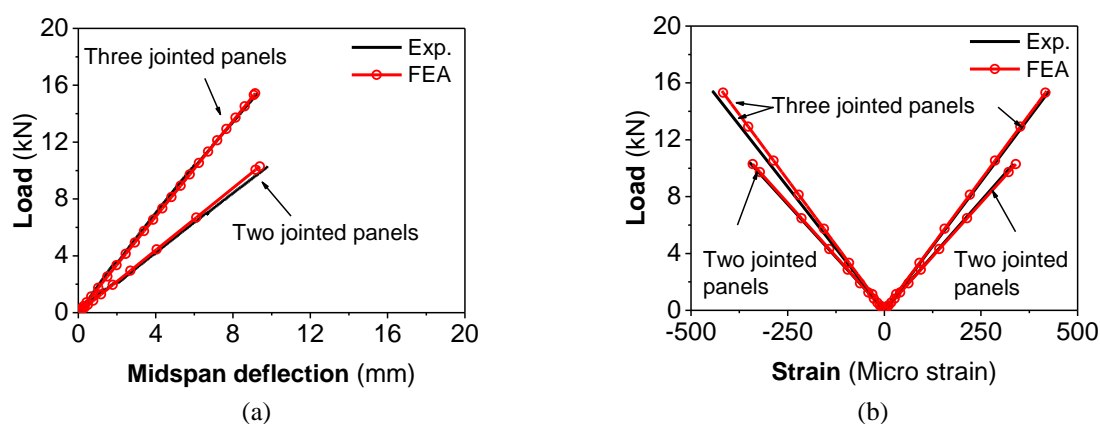
Fig. 9. Experimental *versus* numerical results of jointed panels subjected to ULS loading: (a) load *versus* midspan deflection and (b) load *versus* strain.

4.3. Floor prototype

Table 2 presents the deflection and strain values experimentally measured in the floor prototype, at different monitoring positions, and compares them with the results extracted from the FE simulations. There is a good agreement between the FE model and the experimental test. Average difference in terms of vertical deflection is found to be 1.01, with a Coefficient of Variation (CoV) of 12.40%, while in terms of deformation, average difference is less than a 4% and CoV is 13.00 %.

Table 2. Comparison between experimental and numerical FEM results in the floor prototype.

	Exp.	FE	Exp. / FE
Deflection (mm)			
Midspan of middle panel	33.46	31.01	1.08
Midspan of side panel	20.62	19.33	1.07
Midspan of longitudinal beams	4.60	5.59	0.82
Midspan of transverse beam	13.80	13.08	1.06
		Average	1.01
		CoV	12.40%
Strain (Micro strain)			
Midspan of middle panel	637.53	595.79	1.07
Midspan of side panel	420.08	435.06	0.97
Midspan of longitudinal beams	235.72	301.89	0.78
Midspan of transverse beam	786.19	781.67	1.01
		Average	0.96
		CoV	13.00%

5. Parametric studies and analyses

Several parametrical studies are developed in this section, using the FE models developed and validated in *the* previous section, to delve into the mechanical behaviour of sandwich panels and floor prototype. In all simulations, the constitutive material models and properties were equal to those previously indicated in *section 3*. Besides, loading and boundary conditions were the same as those mentioned above for a single panel, two and three jointed panels and the floor prototype.

5.1. Influence of the U-shaped GFRP profiles

Considering the single sandwich floor panel with the geometry previously indicated, two new cross-sections were proposed (see **Fig. 10**): (i) "U_3" section, in which instead of four U-shaped GFRP profiles, the panel was composed by the two outer U-shaped profiles and one inner U-shaped profile, resulting in a total of 3 U-shaped GFRP profiles; and (ii), "U_2" section, with only the two outer U-shaped profiles.
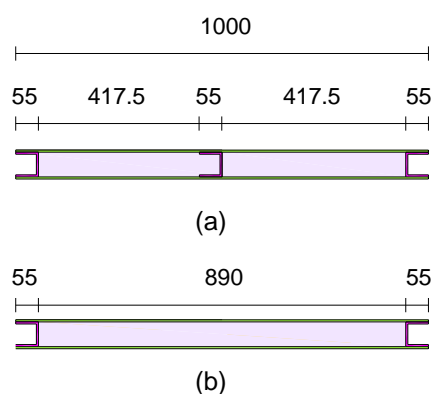

Fig. 10. New cross-sections of the panels considered to study the effect of the U-shaped GFRP profiles: (a) U_3 section; (b) U_2 section.

Results of the new simulations for a single panel and jointed panels under a 4PBT configuration in ULS loading are plotted in **Fig. 11a** and expressed in terms of the maximum midspan deflection *versus* the number of U-shaped profiles. A similar pattern was observed for the three considered cross sections (U_4, U_3 and U_2) in both the single panel and the jointed panels. It was noticed that decreasing the number of U-shaped profiles had a linear consequence in increasing maximum midspan deflection. In this case, decreasing the number of U-shaped GFRP profiles from 4 to 3 and 4 to 2, leads to an increase in the maximum midspan deflection (thus decreasing stiffness) in about 10% and 20%, respectively.

When the simulation was performed on the floor prototype (**Fig. 11b**), decreasing the number of U-shaped

GFRP profiles from 4 to 3 and from 4 to 2, respectively caused an increase of about 10% and 20% in the

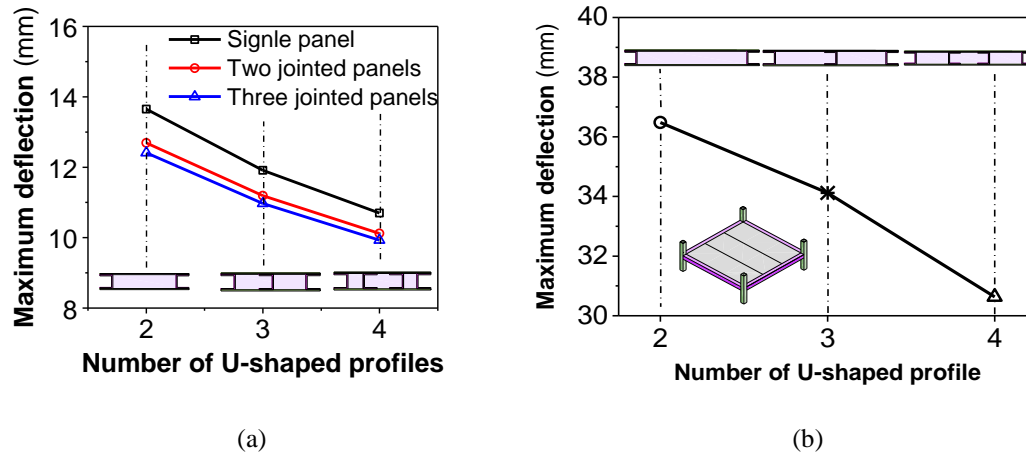maximum deflection registered at the center of the floor slab.

| (a) | (b) |

Fig. 11. Parametric study with U-shaped profile variation: (a) single panel and jointed panels; (b) floor module

Influence of the U-shaped GFRP profiles was also studied in terms of the contribution of shear deformation to

the total deformation [42] at a cross section distanced 250 mm from the free edge of the panels. The results are

listed in **Table 3**. Shear forces were calculated by integration of the shear stresses in the centroid element of

each component, over their respective areas.

Table 3 shows that the number of U-shaped GFRP profiles significantly affects the shear force distribution. On

the opposite, the position of those U-shaped GFRP profiles do not appear to have influence in the shear force

distribution (in panels with 3 and 4 U-shaped GFRP profiles, outer and inner profiles support nearly the same

shear forces). The total contribution of U-shaped GFRP profiles on shear resistance is about 60%, 70% and 80%

for panels U_2, U_3 and U_4, respectively. Therefore, adding one U-shaped GFRP profile led to increase the

contribution of each element in 10%. That reduces the shear contribution of the other elements that form the

panel. The PU foam core is the most affected element when the number of U-shaped GFRP profiles decreases,

as the contribution of core increases. A slightly exponential correlation with the U-shaped GFRP profiles

number can be noticed. Conversely, the contribution of GFRP skins to the shear force resistance is less affected,

and is barely the same when 2 or 3 U shaped profiles are placed in the panels.

Hence, the analyses performed evidence that an optimum mechanical behaviour is obtained when at 3 U-shaped

GFRP profiles are used in the designed sandwich panels. In that case, stiffness is considerably improved and

shear stresses are alleviated from the PU foam core. The use of a fourth U-shaped GFRP profile has a main result of reducing even more shear stresses in the PU foam core.

Table 3. Shear contribution in sandwich panel components with different number of U-shaped GFRP profiles.

Component	Reference panel (U_4 section)		U_3 section panel		U_2 section panel	
	Average shear force (kN)	Relative contribution (%)	Average shear force (kN)	Relative contribution (%)	Average shear force (kN)	Relative contribution (%)
Outer U-shaped profile	1.06	41.63	1.06	41.21	1.50	58.33
Inner U-shaped profile	1.05	40.86	0.67	26.02	0.00	0.00
GFRP skins	0.35	13.62	0.61	23.83	0.61	23.79
PU foam core	0.10	3.89	0.23	8.94	0.45	17.88
Total	2.57	100.00	2.57	100.00	2.57	100.00

5.2. Load distribution and beam-panel connection flexibility

Two new simulations were performed on the floor prototype in order to evaluate the influence of the panel-panel and the beam-panel connections. The first, named "full-connection" model, assumes perfect bond in the panel-beam connection (i.e. considers full composite action by using a tie interface between the squared GFRP profiles and the U-shaped GFRP profiles); and the second, called "continuous-slab" model, defines a continuous slab with dimensions that correspond to the sum of the three jointed panels simulated in the floor prototype. In this last case, top and bottom skins, as well as PU foam, covered 3×3 m^2 without any interruption, U-shaped profiles were placed inside the slab at the same positions that were previously set for the three jointed panels, and since no connection existed, connection profiles between panels were not considered.

Fig. 12 compares the mechanical behaviour of the new simulations with the reference one (i.e. the original FE model) in terms of load *vs* deflection registered at the center of the slabs. All simulated cases follow a linear-elastic relationship between applied load and vertical deflection, but the maximum deflection is clearly different in each one. By estimating stiffness as the slope of the load *vs* deflection curves, it may be found that flexural stiffness is about 30% higher in the continuous slab and about 45% higher in the full-connection model, than in the reference slab.
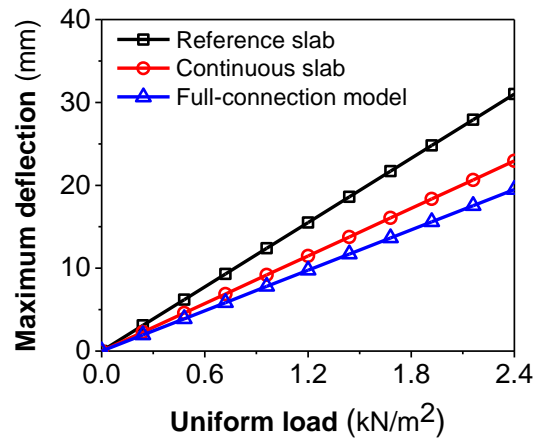
Fig. 12. Load *versus* maximum deflection in the different system proposed

The contour plot representing the vertical displacement (in *y* direction) obtained from FE models is presented in **Fig. 13.** In the case of the reference model, the deflection in the middle panel was 46% higher than the in the side panels. This represents that the middle panel was mainly working in one direction (parallel to panel-panel connections), which is confirmed by the deflection of the beams placed orthogonally to the panel's length: deflection of those beams reached 12.87 mm, while deflection of beams parallel to the panel's length had a deflection of only 6.78 mm. However, in the case of the continuous-slabs and full-connection model, the deflection of the middle panel is only 35% higher than the deflection in the side panels, and the flooring system showed a two-way slab behaviour. That confirms the mentioned predominant behaviour of the prototype in one direction, which is explained by the existence of the U-shaped profiles and by the type of the connection to the side panels.
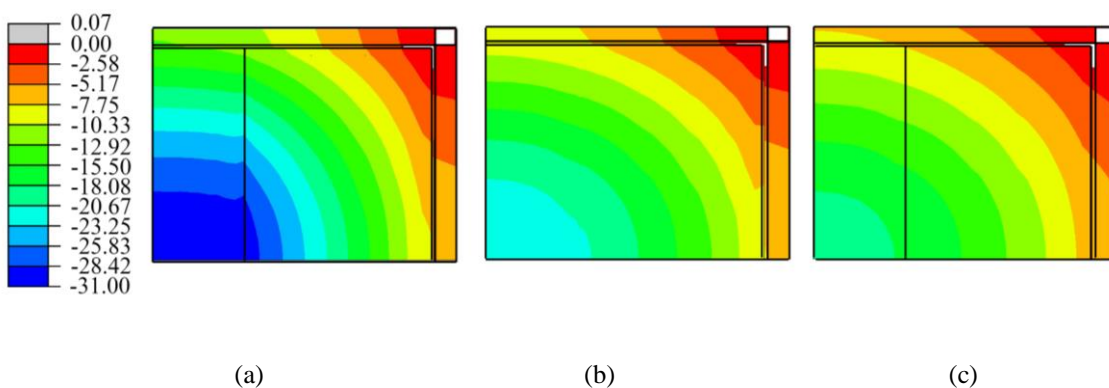

(a)   (b)   (c)

Fig. 13. Vertical deflection contour plots (in mm) for: (a) reference slab composed by three jointed panels; (b) continuous-slab model; (c) full-connection model.

Moreover, stresses developed at the external faces of bottom and top GFRP skins of the reference prototype are

shown in **Fig. 14**. The difference of stress distribution at the middle of the panels and through their edges

evidence that panels are working as two-way slabs, and the longitudinal direction is the main working direction.
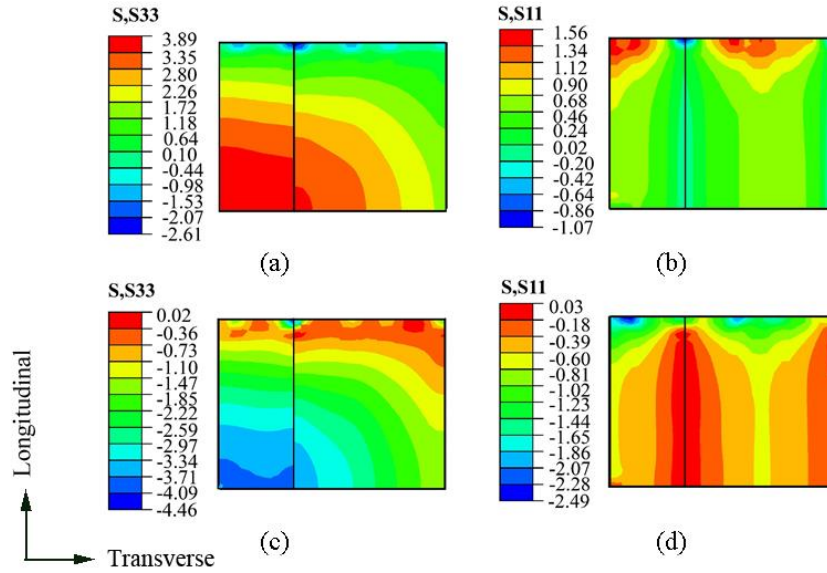

Fig. 14. Distribution of stress in the GFRP skins of the reference prototype: (a) longitudinal direction-bottom skin; (b) transverse direction-bottom skin; (c) longitudinal direction-top skin; (d) transverse direction-top skin (stresses, in MPa).

Fig. 14 shows that the proposed connection system provides some amount of unknown restriction along the

supports which consequently contributes to reduce the overall floor flexibility. It can be seen that the type of

connection used does not act as a fully fixed support and thus, works as a semi-fixed connection. Accordingly,

the total deflection at panels midspan joint (δ) would be the sum of the deflection due to the fixed support

(δ_{FC}) and the connection flexibility (δ_θ), defined in Eq. (4).

$$\delta = \delta_{FC} + \delta_\theta \tag{4}$$

The stiffness, defined as the slope between load and deflection, may be expressed by Eq. (5):

$$\frac{k_{FC}}{k_{PC}} = \frac{\delta}{\delta_{FC}} \tag{5}$$

where k_{FC} is the stiffness of panel in full connection (FC) model, k_{PC} is the stiffness of panels in semi-fixed

(PC) support conditions.

Eq. (5) could be modified in other term as Eq. (6), where Π is the stiffness reduction factor.

$$\frac{k_{PC} + \Pi \times k_{FC}}{k_{PC}} = \frac{\delta_{FC} + \delta_{\theta}}{\delta_{FC}} \tag{6}$$

Based on **Fig. 12**, coefficient Π was calculated to be 0.60. Thus, when using the proposed connection in the prototype, which acts as a semi-fixed support conditions, a stiffness reduction of a 60% respect to a fixed support condition can be expected.

5.3. Influence of the aspect ratio and of the slenderness ratio

Sandwich panel aspect ratio, r, is defined as L/w, where L and w are the panel's length and width, respectively. Slenderness ratio, r_s, is defined as h/w, being h the height of the sandwich panel. Both parameters have significant impact on the stiffness and on the deformability of the sandwich floor panel. They also have an impact on economic aspects of the floor prototype developed: changing the slenderness ratio enables exploring the variation of stiffness with a minimum cost, since PU foam is the less expensive constituent of the system. Aspect ratio variations relate the deformational response of the panels with their transport costs (due to dimensions).

New simulations, varying both the aspect ratio and the slenderness ratio, were conducted. In general, maintaining the width of the panels constant contributes to not changing significantly the transport conditions. Therefore, this dimension was kept constant and equal to 1 m in all simulations. The values considered for the panels span length were 1.0 m, 1.5 m, 2.0 m, 2.5 m, 3.0 m, 3.5 m and 4.0 m, which result in aspect ratio values of 1.0, 1.5, 2.0, 2.5, 3.0, 3.5 and 4.0, respectively. Similarly, the thickness of GFRP skins, was kept constant and equal to 5 mm in all simulations, because this material is significantly more expensive than PU foam core. Values considered for PU foam thickness were 60 mm, 80 mm and 100 mm, which leads to panels with a total height of 70 mm, 90 mm and 110 mm and results in slenderness ratio values of 0.07, 0.09 and 0.11, respectively.

Additionally, the connection conditions between GFRP beams elements and sandwich floor panels were evaluated for the following two scenarios: (i) semi-fixed (i.e. like the actual one on the experimentally tested prototype) with the designation of 'PC'; (ii) fixed connection, called 'FC'.

A total of 42 models were created and analysed under ultimate load conditions in residential buildings by assuming a uniform distributed load of 2.4 kN/m^2 on the top surface of the sandwich floor panels. Selected representative results are indicated in Error! Reference source not found..

Table 4. Maximum predicted longitudinal strain in the proposed residential floor system, under an ultimate uniform load of 2.4 kN/m^2

| $r_s = h/w$ | $r = L/w$ | Longitudinal maximum strain (µε) | | | | | | | |
| | | Middle of middle panel | | Middle of side panel | | Longitudinal beam | | Transverse beam | |
		PC	FC	PC	FC	PC	FC	PC	FC
0.07	1	92.4	91.8	71.8	84.9	19.8	16.9	274.0	228.8
	2	324.1	222.3	216.3	174.7	106.1	121.7	532.9	414.0
	3	595.8	353.6	435.1	280.7	301.9	307.3	781.7	555.5
	4	881.6	523.0	664.2	395.3	613.8	570.9	1043.0	644.6
0.09	1	71.3	59.1	57.0	66.0	20.4	13.1	259.7	207.9
	2	239.0	175.7	172.5	157.3	94.1	99.0	503.6	365.7
	3	458.5	305.8	368.9	283.5	255.1	256.6	722.2	479.5
	4	733.4	480.3	610.8	440.6	502.3	469.1	966.4	559.6
0.11	1	62.0	41.3	47.6	56.1	22.5	8.0	250.3	180.6
	2	200.4	144.4	148.8	141.5	77.3	76.8	493.2	309.3
	3	396.9	268.4	330.4	274.6	193.7	201.8	710.0	399.7
	4	662.1	448.7	571.5	459.6	388.5	372.5	967.9	459.0

h_c : PU foam core thickness; h_f : skin thickness; L : length of the floor panel; w : width of the floor panel;

r_s : slenderness ratio; r : aspect ratio; PC: semi-fixed connection; FC: fixed connection

Error! Reference source not found. reveals that, in all cases, the maximum strain values in the residential floor system under ultimate uniform load are significantly below the ultimate strains obtained in the material characterization. It can be seen that the maximum strain is always occurring in the transverse beam. On the other hand, increasing the slenderness ratio leads to a reduction on the maximum strain in different components, due to contribution of the flexural stiffness of the panel.

Increasing the slenderness ratio from 0.07 to 0.11 in the shortest panels (*L=1000 mm*) provided a decrease in the maximum strain that varied between 45% and 65% when the four considered components of the panel and two connection conditions are analysed. In this case, the highest decrease occurred in the modular system with 'FC' connection. However, the range of the aforementioned values is altered with the increase of panel's aspect ratio, varying between 63% and 82% in the longest panels (*L=4000 mm*).
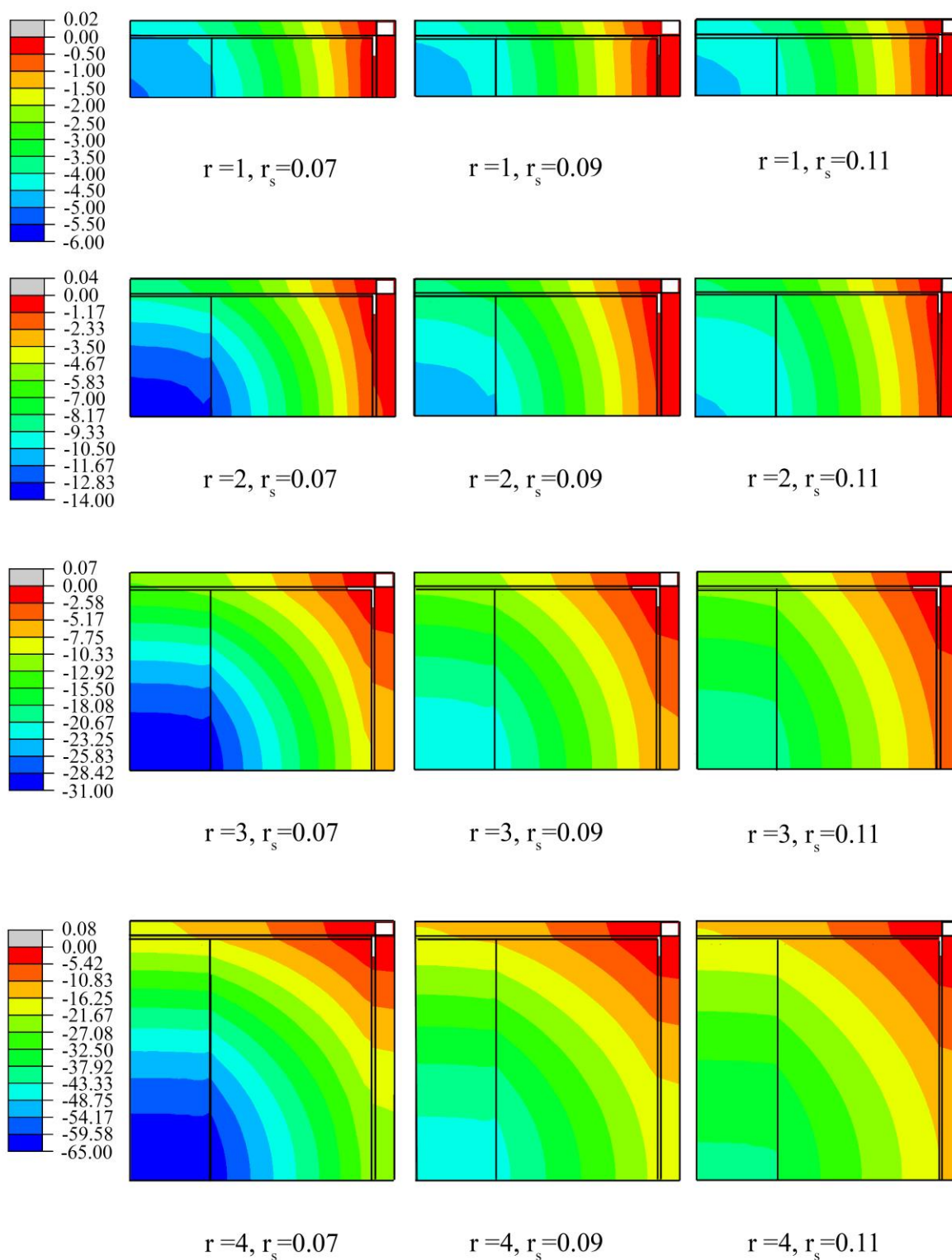
Fig. 15. Vertical deflection of the residential floor modular system, considering different slenderness and aspect ratios, with 'PC' support condition (values in mm).

Predicted vertical deflection of the residential floor system under different slenderness and aspect ratios with 'PC' support conditions is depicted in **Fig. 15.** In all cases, the maximum deflection occurred at the center of the middle panel. Increasing geometrical aspect ratio range from 1 to 4 leads to an increase in the maximum middle span deflection. Conversely, increasing slenderness ratio results in decreasing the maximum midspan deflection. In this case, the highest deflection occurred in the modular system with geometrical aspect ratio and slenderness ratio of 4 and 0.07, respectively.

The Italian standard CNR [43] is commonly used to verify the performance of composite sandwich panels under service conditions. Accordingly, the maximum deflection registered in long term for the quasi-permanent load (equal to 30% of the service load) should be less than *L/250*. Deflection in long term for a panel (δ_{LT}) can be estimated as:

$$\delta_{LT} = \alpha \times \delta_{SLS} \times \gamma_{Creep} \tag{7}$$

where, δ_{SLS} is the deflection corresponding to the service condition (in this case, for a uniform distributed load of 1.6 kN/m^2) , α is the proportion of the load in quasi-permanent load respect to load in service (i.e. 30%), and γ_{Creep} is an estimated coefficient due to effects of creep.

Computed results of a creep test previously developed on the studied sandwich panels [44] yielded an increment of a 252% in the deflection of panels due to viscoelastic effects after the 5 years assumed to be the service life of the structure. Hence, value for coefficient γ_{Creep} can be set to 2.52 in this investigation.

For each of the 42 model studied, the deflection corresponding to long term can be computed based on Eq. (7). It should be mentioned that since floor sandwich panels are supported on exterior beams, comparison to the standard prescribed value should be done by subtracting deflection of those exterior beams. Obtained results are depicted in the **Fig. 16**. Results in this figure are based on: (i) the aspect ratio; (ii) the slenderness ratio; and (iii) the type of the connection between GFRP beam's elements and sandwich floor panels.
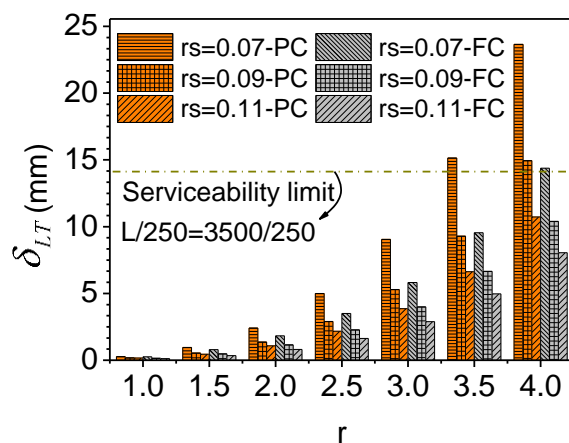
Fig. 16. Predicted long term deflection in floor panel modular system.

Fig. 16 could be utilized in the preliminary design of composite sandwich panels to be applied in residential buildings. In this figure, maximum deflection criterion recommended by CNR [43] is plotted by horizontal dotted lines. Accordingly, all of the proposed panels except than the panel designated by 0.07-SC could be selected.

Fig. 16 also shows that in some geometrical aspect ratios, the predicted maximum long term deflection of the proposed residential pavement is much lower than the serviceability limit criteria. This shows a possible overdesign of the modular system, which may be put down. Thus, a study that indicates when to reduce the number of U-shaped GFRP profiles from 4 profiles to 3 and from 3 to 2 profiles is interesting to carry out. Hence, in a similar way as indicated in the case of floor prototype with 4 U-shaped profile, 84 models were studied for the floor prototypes with presence of 3 and 2 U-shaped profiles. The deflections correspondent to the long term with respect to the aspect ratios and slenderness ratios are depicted in **Fig. 17**.
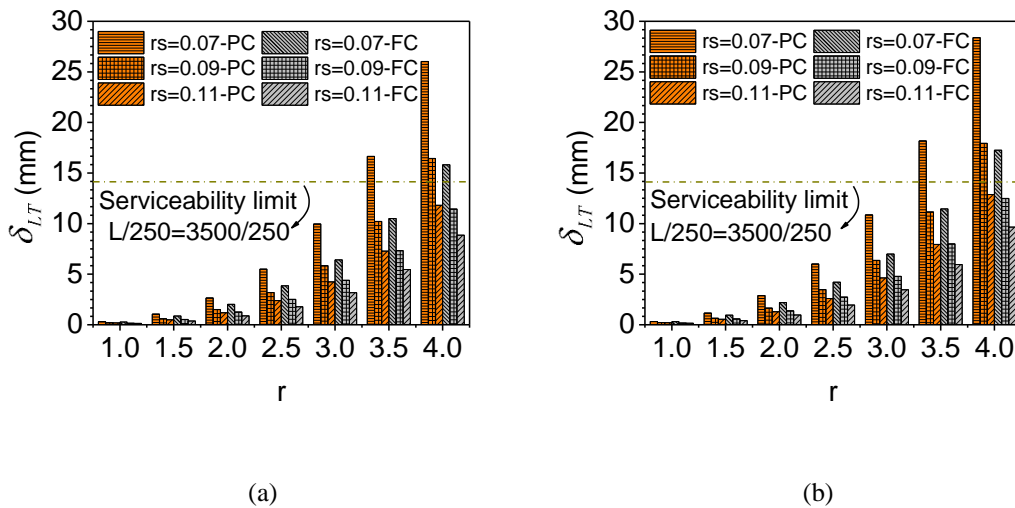
Fig. 17.Floor prototype with variation of U-shaped profiles: (a) 3 U-shaped profile; (b) 2 U-shaped profile.

4. Conclusions

This paper has presented a FE model developed to simulate the mechanical behavior of a floor module prototype to be use in a temporary emergency house. The FE model has taken into account geometrical and material nonlinearities and adherent surfaces interaction, and has been calibrated and validated based on a series of experimental tests performed previously on the mentioned floor prototype and its different components. Several numerical parametric studies were conducted to analyze the influence of placing internal ribs on the sandwich panels, the flexibility of the connection between panels and the frame structure, and the influence of aspect ratio and slenderness ratio of the panels. Based on that, the following conclusion may be drawn:

1- The developed FE model is able to accurately reproduce the mechanical behavior of the prototype experimentally studied, as well as the behavior of a single panel and two and three panels working together. The numerical simulation considering "crushable foam" model in the PU foam core and an interface model with cohesive behavior for simulating the adherent surfaces between the different components of a panel, gives a reasonable outcome, and is capable of capturing the failure mode of a single panel. Failure occurred in the compression GFRP skin due to outward local buckling failure mode in the region of the loading. The obtained failure evidences that the skin-core interaction has a major effect on the flexural performance of the sandwich panel and cannot be neglected.

2- The importance of utilizing U-shaped GFRP profiles for increasing flexural stiffness of the composite sandwich panel is clearly observed. In the case of single, two jointed panels and modular prototype,

decreasing the number of those U-shaped GFRP profiles from 4 to 3 and 2 results in decreasing flexural stiffness by 10% and 20%, respectively.

3- The number of U-shaped GFRP profiles also has influence on the contribution of composite sandwich panel's components in distributing shear forces. Total contribution on shear resistance of U-shaped GFRP is about 60%, 70% and 80 % when 2, 3 and 4 U-shaped profiles, respectively, are placed in the panel. U-shaped GFRP profiles mainly alleviate shear stresses from the PU foam core, being GFRP skins contribution to the shear force resistance less affected by the number of U-shaped GFRP profiles used.

4- The floor prototype presents a predominant behaviour in one direction, especially in the parallel to panel-panel connections direction. Stress distribution also evidences that phenomenon, which may be explained due to the existence of the U-shaped profiles inside panels and on the connection of a panel with the other panels and beams.

5- Designed beam-panel connection results in a semi-fixed support conditions for the panels, and a stiffness reduction of a 60% respect to a fixed support condition (i.e. if a tie connection existed between beams and panels) can be expected.

6- Sandwich panel aspect ratio and slendenessr ratio have a significant impact on the stiffness and the deformability of the sandwich panel, as well as on economic issues. Higher aspect ratios increase transport cost, and also tend to result in high deformations. Slenderness ratio variation enables exploring an optimum value of stiffness with a minimum cost. Moreover, both ratios are not independent. Hence, registered strains in the prototype vary between 45% and 65% when modifying slenderness ratio for a small values of the aspect ratio, but those values increase to 63% and 82% for a large value of the aspect ratio.

7- Due a lack of specific designing codes for analyzing complex modular residential pavement system, a specific chart has been developed to be used in the design of sandwich panels similar to those used in the modular system presented, taking into account several values of slenderness and geometrical aspect ratios.

Acknowledgements

References

[1] Hou S, Shu C, Zhao S, Liu T, Han X, Li Q. Experimental and numerical studies on multi-layered corrugated sandwich panels under crushing loading. Composite Structures. 2015;126:371-85.

[2] Veljkovic M, Johansson B. Light steel framing for residential buildings. Thin-Walled Structures. 2006;44:1272-9.

[3] Pelletier JL, Vel SS. Multi-objective optimization of fiber reinforced composite laminates for strength, stiffness and minimal mass. Computers & Structures. 2006;84:2065-80.

[4] Allen GH. Analysis and Design of Structural Sandwich Panels. . London: Pergmon Press, 1969.

[5] Davies JM. Lightweight Sandwich Construction. . Wiley-Blackwell; 2001.

[6] D'Alessandro V, Petrone G, Franco F, De Rosa S. A review of the vibroacoustics of sandwich panels: Models and experiments. Journal of Sandwich Structures and Materials. 2013;15:541-82.

[7] Belouettar S, Abbadi A, Azari Z, Belouettar R, Freres P. Experimental investigation of static and fatigue behaviour of composites honeycomb materials using four point bending tests. Composite Structures. 2009;87:265-73.

[8] Russo A, Zuccarello B. Experimental and numerical evaluation of the mechanical behaviour of GFRP sandwich panels. Composite Structures. 2007;81:575-86.

[9] Shawkat W, Honickman H, Fam A. Investigation of a novel composite cladding wall panel in flexure. Journal of Composite Materials. 2008;42:315-30.

[10] Sharaf T, Shawkat W, Fam A. Structural performance of sandwich wall panels with different foam core densities in one-way bending. Journal of Composite Materials. 2010;44:2249-63.

[11] Correia JR, Garrido M, Gonilha JA, Branco FA, Reis LG. GFRP sandwich panels with PU foam and PP honeycomb cores for civil engineering structural applications: Effects of introducing strengthening ribs. International Journal of Structural Integrity. 2012;3:127-47.

[12] Keller T, Haas C, Vallé T. Structural concept, design, and experimental verification of a glass fiber-reinforced polymer sandwich roof structure. Journal of Composites for Construction. 2008;12:454-68.

[13] Mousa MA, Uddin N. Global buckling of composite structural insulated wall panels. Materials & Design. 2011b;32:766-72.

[14] Ginjeira do Nascimento J. Transitional architecture in emergency scenarios. Clickhouse case study: modular shelter made of advanced composite materials. Portugal: Técnico Lisboa, 2015.

[15] Garrido M, Correia JR, Keller T, Branco FA. Adhesively bonded connections between composite sandwich floor panels for building rehabilitation. Composite Structures. 2015;134:255-68.

[16] Abdolpour H, Garzón-Roca J, Escusa G, Sena-Cruz JM, Barros JAO, Valente IB. Development of a composite prototype with GFRP profiles and sandwich panels used as a floor module of an emergency house. Composite Structures. 2016;153:81-95.

[17] Keller T, Rothe J, de Castro J, Osei-Antwi M. GFRP-Balsa Sandwich Bridge Deck: Concept, Design, and Experimental Validation. J Compos Constr. 2014;18:04013043.

[18] Liu Z, Majumdar P, Cousins T, Lesko J. Development and Evaluation of an Adhesively Bonded Panel-to-Panel Joint for a FRP Bridge Deck System. J Compos Constr. 2008;12:224–33.

Abdolpoura, H.; Garzón-Roca, J.; Sena-Cruz, J.; Barros, J.A.O.; Valente, I. (2020) "FEM based numerical strategy for the analysis of composite modular floor prototype for emergency housing applications." Journal of Structural Engineering, 146(1): 04019172 1–14.
DOI: 10.1061/(ASCE)ST.1943-541X.0002459

[19] Turner MK, Harries KA, Petrou MF, Rizos D. In situ structural evaluation of a GFRP bridge deck system. Composite Structures. 2004;65:157-65.

[20] Zhou A, Keller T. Joining techniques for fiber reinforced polymer composite bridge deck systems. Composite Structures. 2005;69:336-45.

[21] Mara V, Al-Emrani M, Haghani R. A novel connection for fibre reinforced polymer bridge decks: Conceptual design and experimental investigation. Composite Structures. 2014;117:83-97.

[22] Ha KH. Finite element analysis of sandwich plates: An overview. Computers & Structures. 1990;37:397-403.

[23] Thomsen OT. Analysis of local bending effects in sandwich plates with orthotropic face layers subjected to localised loads. Composite Structures. 1993;25:511-20.

[24] Glenn CE, Hyer MW. Bending behavior of low-cost sandwich plates. Composites Part A: Applied Science and Manufacturing. 2005;36:1449-65.

[25] Demiray S, Becker W, Hohe J. A triangular v. Kármán type finite element for sandwich plates with transversely compressible core. Computer Methods in Applied Mechanics and Engineering. 2004;193:2239-60.

[26] Tuwair H, Hopkins M, Volz J, ElGawady MA, Mohamed M, Chandrashekhara K, et al. Evaluation of sandwich panels with various polyurethane foam-cores and ribs. Composites Part B: Engineering. 2015;79:262-76.

[27] Mostafa A, Shankar K, Morozov EV. Behaviour of PU-foam/glass-fibre composite sandwich panels under flexural static load. Materials and Structures/Materiaux et Constructions. 2014:1-15.

[28] Awad ZK, Aravinthan T, Zhuge Y. Experimental and numerical analysis of an innovative GFRP sandwich floor panel under point load. Engineering Structures. 2012;41:126-35.

[29] Mitra N, Raja BR. Improving delamination resistance capacity of sandwich composite columns with initial face/core debond. Composites Part B: Engineering. 2012;43:1604-12.

[30] Abdolpour H, Escusa G, Sena-Cruz JM, Valente IB, Barros JAO. Axial Performance of Jointed Sandwich Wall Panels. Journal of Composites for Construction. 2017:12.

[31] Abdolpour H, Garzón-Roca J, Escusa G, Sena-Cruz JM, Barros JAO, Valente IB. Composite modular floor prototype for emergency housing applications: Experimental and analytical approach. Journal of Composite Materials. 2017:0021998317733318.

[32] UNHCR. United Nations High Commissioner for Refugees Supply Management Service HQSF00. Budapest, Hungary2010.

[33] Standardization ECf. Eurocode 0: Basis of structural design. Technical Committe CEN/TC 250, Brussels; 1990.

[34] ASTM. Standard Test Method for Flexural Properties of Sandwich Constructions. ASTM C393. United States

West Conshohocken, PA 19428-2959

2000.

[35] ABAQUS. The numerical model was performed in collaboration with the Department of Construction Engineering of the Universitat Politècnica de València . 6.12 ed.

[36] Deshpande VS, Fleck NA. Isotropic constitutive models for metallic foams. Journal of the Mechanics and Physics of Solids. 2000;48:1253-83.

[37] Wang W. Cohesive Zone Model for Facesheet-Core Interface Delamination in Honeycomb FRP Sandwich Panels: Morgantown, West Virginia, 2004.

[38] Westergaard HM. Bearing pressures and cracks. Transactions of the American Society of Mechanical Engineers. 1939;61:A49-A53.

[39] Mousa MA, Uddin N. Flexural behavior of full-scale composite structural insulated floor panels. Advanced Composite Materials. 2011a;20:547-67.

[40] Zenkert D. The Handbook of Sandwich Construction. London, United Kingdom: Chameleon Press Ltd., 1997.

[41] Carlsson LA, Kardomateas GA. Structural and Failure Mechanics of Sandwich Composites. New York Springer, 2011.

[42] Fam A, Sharaf T. Flexural performance of sandwich panels comprising polyurethane core and GFRP skins and ribs of various configurations. Composite Structures. 2010;92:2927-35.

[43] Council INR. CNR, Guide for the Design and Construction of Structures made of FRP Pultruded Elements. ROME2008.

[44] Abdolpour H, Garzón-Roca J, Sena-Cruz J, escusa G. Experimental and Numerical Mechanical Behavior of Composite Structure to be used as the Floor of an Emergency House Prototype: Part II-Numerical. Composite Structures. 2015.

Abdolpoura, H.; Garzón-Roca, J.; Sena-Cruz, J.; Barros, J.A.O.; Valente, I. (2020) "FEM based numerical strategy for the analysis of composite modular floor prototype for emergency housing applications." Journal of Structural Engineering, 146(1): 04019172 1–14.
DOI: 10.1061/(ASCE)ST.1943-541X.0002459